

An Ultrafast Phase Modulator for 3D Imaging

Janice Y. Cheng^a and Qiushui Chen^b

^aElectrical and Computer Engineering Department, Northeastern University,
360 Huntington Ave. , Boston, MA, USA 02115;

^bBoston Applied Technology, Inc., 6F Gill Street, Woburn, MA, USA 01801

ABSTRACT

In this paper we explore potential applications of a new transparent Electro-Optic Ceramic in 3D imaging as a fast phase shifter and demonstrate its performance in a newly developed Low Coherence Polarization Interference Microscopy (LCPIM). The new phase modulator is fast, convenient and inexpensive. It makes the 3D imaging system that employs it mechanically efficient and compact. The LCPIM proposed in this paper has the advantages of rapid phase shifting and adjustable reference/objective intensity ratio for maximum contrast. The new phase modulator has been approved feasible by several experiments.

Keywords: Phase Modulator, Interference Microscopy, 3D Imaging, Low Coherence, Ceramic Material

1. INTRODUCTION

Interference-based three dimensional (3D) imaging techniques, such as White Light Interferometry(WLI)¹ , Optical Coherence Tomography(OCT)² , and Digital Phase-Shifting Holography(DPSH)³ , have drawn a significant amount of attention of researchers and will continue to be a hot topic in both academia as well as industry. Interference-based 3D imaging techniques rely on an accurate rate of change of the optical path difference between the object and reference beams to record the object information. Therefore optical phase modulators that introduce the variational phase difference play an important role in these techniques.

Many phase modulator designs have been introduced in the literature. One of the most popular of these is mechanical translating of a reference mirror by the movement of a stepping motor or a piezoelectric transducer. This scheme is low-cost and easy to apply and has frequently been used in commercial WLI and OCT instruments^{1,4} . The other widely used technique of phase shifting is called geometric phase modulation, which is based on polarization optics⁵ or uses a frequency domain optical delay line⁶ . An achromatic phase shift is possible in this method. More recently in ⁷ , the author proposed a phase shifter using two acousto-optic modulators. This latter phase shifter can directly control the phase of a collimated beam and is insensitive to the polarization of the incident beam when polarization-insensitive AOMs are used. Unlike the other two methods there is no mechanical movement involved in this design. However, the 3D imaging system that uses this phase modulator is going to be mechanically complicated and expensive.

In this paper we introduce a new phase modulator made by a newly developed electro-optic transparent ceramic material called $Pb(Mg_{1/2}Nb_{2/3}O_3-PbTiO_3)$ (PMN-PT)⁸ . The new phase shifter, here after referred as the Ceramic PM (phase modulator), introduces phase variation based on an Electro-optic effect. We will show later in the paper that the Ceramic PM is an excellent alternative to conventional phase shifters. In particular, it has a much faster response speed than any of the standard phase modulators and, by working either alone or together with other phase shifters, it is able to meet the demand of fast phase shifting of "video rate" 3D

Further author information: (Send correspondence to Janice Y. Cheng)

Janice Y. Cheng: E-mail: ycheng@coe.neu.edu, Telephone: 1 617 373 7791

Qiushui Chen: E-mail: qchen@bostonati.com, Telephone: 1 781 935 2800

imaging. The interference-based imaging system that utilizes Ceramic PM does not cost much more than that using a mechanical phase modulator and has the advantages of no moving-parts and compactness.

To study the possibility of using the Ceramic PM in 3D imaging, a novel low-coherence polarization interference microscope, hereafter called LCPIIM, has been developed. Low coherence interference microscopy combines an interferometer and microscopy into one instrument and is able to image 3D micro engineering surface structures⁴. In its usual operation the object is scanned along the vertical axis (z axis) by a piezoelectric translation stage and good contrast fringes will be obtained only when the optical path difference between the two paths of the interferometer is approximately zero. Different types of architecture based on the Mirau correlation microscope⁴, the Linnik microscope⁵ and the Michelson interferometer⁹ have been discussed in the literature. Our design of LCPIIM employs Michelson interferometer objective and is different from the conventional interference microscope in two novel ways: (1) the time consumption on phase shifting is dramatically decreased and (2) the object/reference intensity ratio is adjustable.

This paper is arranged as follows. In section 2 we discuss the properties of PMN-PT material and elaborate the advantages of Ceramic PM as a phase modulator in 3D imaging. The schematic design of the LCPIIM and integrals processing method is introduced in section 3. Section 4 is devoted to presenting several experimental results. Section 5 contains a summary of the results obtained in the paper and suggestions for future work.

2. ELECTRO-OPTIC CERAMIC PHASE MODULATOR

2.1. The PMN-PT Material

It is important to understand the properties of the ceramic material PMN-PT of which our Ceramic PM is constructed before we go into any details of its operation. This material belongs to the OptoCeramic discipline, which is a family of transparent oxide electro optic ceramic materials. PMN-PT has an isotropic minimum energy stable structure and exhibits birefringence in response to an electric field. Compared to crystal materials it features high EO effect, good transparency, ceramic ruggedness and low cost.

PMN-PT is a quadratic Kerr electro-optic material. The change of its refractive index is proportional to the square of the electric field. The amount of the phase retardation of PMN-PT can be parameterized by

$$\Gamma = \frac{\pi t n^3 R E^2}{\lambda} \quad (1)$$

where R is the electro-optic coefficient, n is the optical refractive index of the material, λ is the wavelength of the incident light and t is the distance that the light travels inside the material. Figure (1) illustrates measured phase retardance (phase shift) vs. applied field on a PMN-PT sample with thickness $t = 0.45mm$ at the wavelength of $\lambda = 1.55\mu m$. High EO effect of the material implies activation loss is negligible with minimized electric field induced scattering from the material.

The response time of PMN-PT is very short: in the range of sub-microsecond. The electron and ion movements responsible for the EO effect of the material are much faster than that of molecular movement in liquid crystal materials. Figure (2) shows that the switching speed of the Ceramic PM discussed in this paper is about $500ns$.

2.2. Ceramic PM in 3D Imaging

There are a number of reasons to believe that the Ceramic PM made from PMN-PT will find its way in 3D imaging. High EO effect of the material means that no high voltage supply is required, which is very important in commercial instrumentation. With mature hot-pressing technique, it is much easier and cheaper to make than crystal phase modulator. The positioning of the Ceramic PM is flexible and it will add no additional instrumental complication. The imaging system is less sensitive to the environment because there is no movement of Ceramic

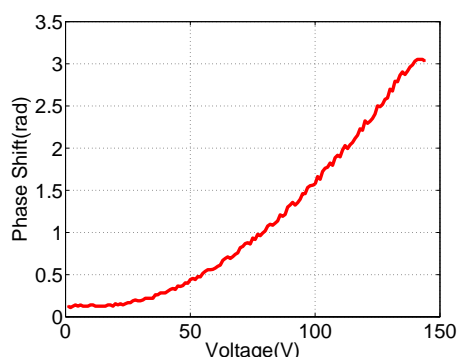


Figure 1. Measured phase retardance (phase shift) vs. applied field of a PMN-PT sample with thickness= 0.45mm at wavelength $\lambda = 1.55\mu m$

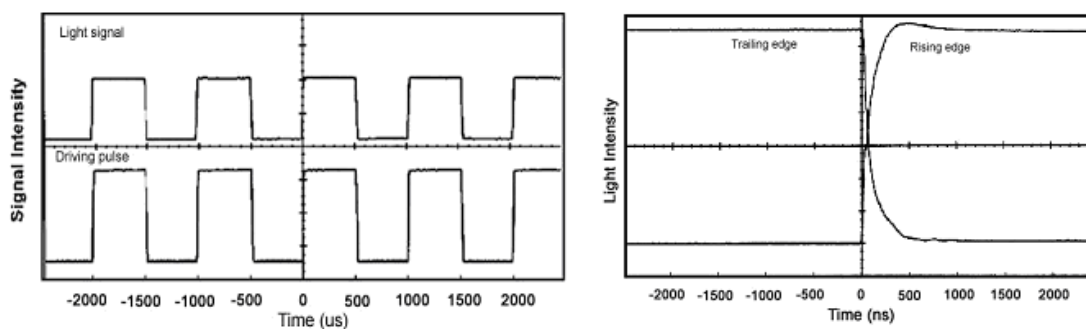


Figure 2. The response speed of the Ceramic PM discussed in this paper

PM during the phase shifting process. In advanced 3D imaging "video-rate" implies 15 frames/sec, which demands that the generation time of each 3D image should be no more than 0.0667 seconds. A data acquiring process has to be accomplished during such a short period of time which involves at least 4 phase shifts for the simplest system. With response time less than $1\mu s$, the new phase shifter is best suited for this situation.

The Ceramic PM modulates the phase by electrically introducing retardation between ordinary and extraordinary wavefronts. So the device configuration illustrated in Figure (3) is required for the polarization interferometric imaging system that uses Ceramic PM. We now take a close look at how polarization states of the incident light change after propagation through each device. *Jones Vectors* are used for analysis in the following and intensity coefficients will be dropped for simplicity. Linear polarizer A, which makes a 45° angle with the \hat{x} axis specified in figure (3), transforms the input random polarized light into linear polarized light of stage (a). The linear polarized light is then directed to an interference system with polarized beam splitter and turns to two orthogonally polarized beams J_x^b and J_y^b at stage (b):

$$J_x^b = \exp^{-i\phi} \begin{bmatrix} 1 \\ 0 \end{bmatrix}; J_y^b = \begin{bmatrix} 0 \\ 1 \end{bmatrix}$$

where ϕ is the phase difference between the object and reference beam. After the two beams go through the Ceramic PM, whose fast axis is aligned with the polarization state of one of the orthogonal polarized beams, the

Jones Vectors of the beams are:

$$J_x^c = \exp^{-i\phi} \begin{bmatrix} 1 \\ 0 \end{bmatrix}; J_y^c = \begin{bmatrix} 0 \\ \exp^{-i\Gamma} \end{bmatrix}$$

The object beam remains unchanged and the reference beam acquires a phase shift of Γ , where Γ is the electronically controlled phase retardation of eq.(1). The two beams will be combined together and form fringes by linear polarizer B, whose transmission axes makes a 45° angle with the fast axis of Ceramic PM. The *Jones Vectors* representation of stage (d):

$$J_x^d = \exp^{-i\phi} \begin{bmatrix} 1/2 \\ 1/2 \end{bmatrix}; J_y^d = \begin{bmatrix} 1/2 \exp^{-i\Gamma} \\ 1/2 \exp^{-i\Gamma} \end{bmatrix}$$

The real part of the inner product of the two beams is:

$$\Re(J_x^d, J_y^d) = \frac{1}{2} \cos(\phi - \Gamma) \quad (2)$$

which indicates that the fringes formed by the device combination carries the object information and phase shift value .

The linear polarizer-polarized beam splitter-linear polarizer combination makes the reference/objective intensity ratio adjustable. We just need to rotate the linear polarizer A for maximum fringe contrast. This design is especially useful for imaging weak scattering object such as biological tissues and therefore has great potential of being applied in medical imaging.

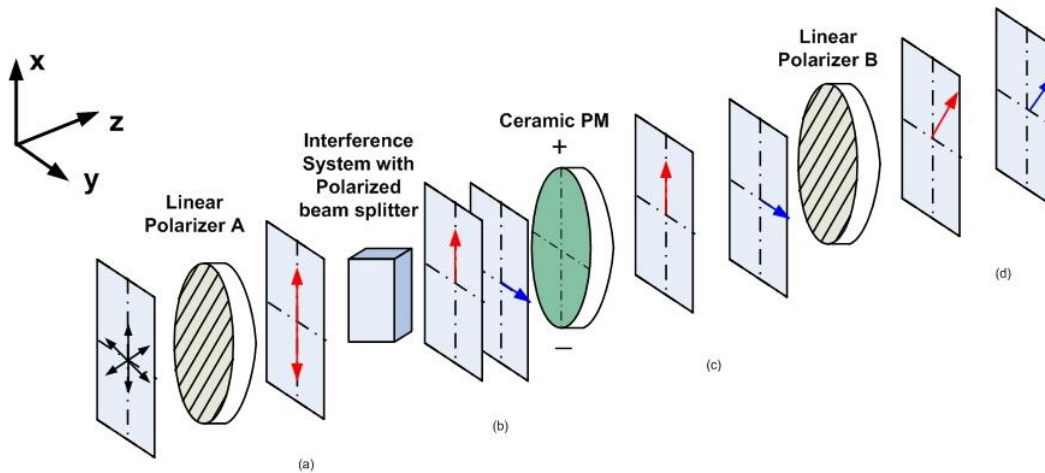


Figure 3. The change of polarization state of incident light after it travels through the imaging system

3. LOW COHERENCE POLARIZATION INTERFERENCE MICROSCOPY

3.1. Hardware

In order to test the feasibility of Ceramic PM as a phase shifter, we developed a Low Coherence Polarization Interference Microscope. Figure(4) illustrates the schematic diagram of the new LCPIM using Ceramic PM. It is constructed based on the device combination introduced in section (2.2) and uses a Michelson interferometric objective design. The light generated by a broad band source is condensed and transmitted through the linear

polarizer *A*. The polarized beam is then divided by a beam splitter. One of the beams is directed into a microscope objective and is immediately separated at a polarizing beam splitter into two orthogonally polarized beams. After reflection at the reference mirror and the testing object, these beams return along their original paths to the beam splitter. They then go through the Ceramic PM and the linear polarizer *B* and are focused by an eyepiece to a small area before forming a pattern of light and dark interference "fringes" at the CCD camera. The "fringes" carry the information of the testing object and the 3D object can be retrieved after the acquired data is processed.

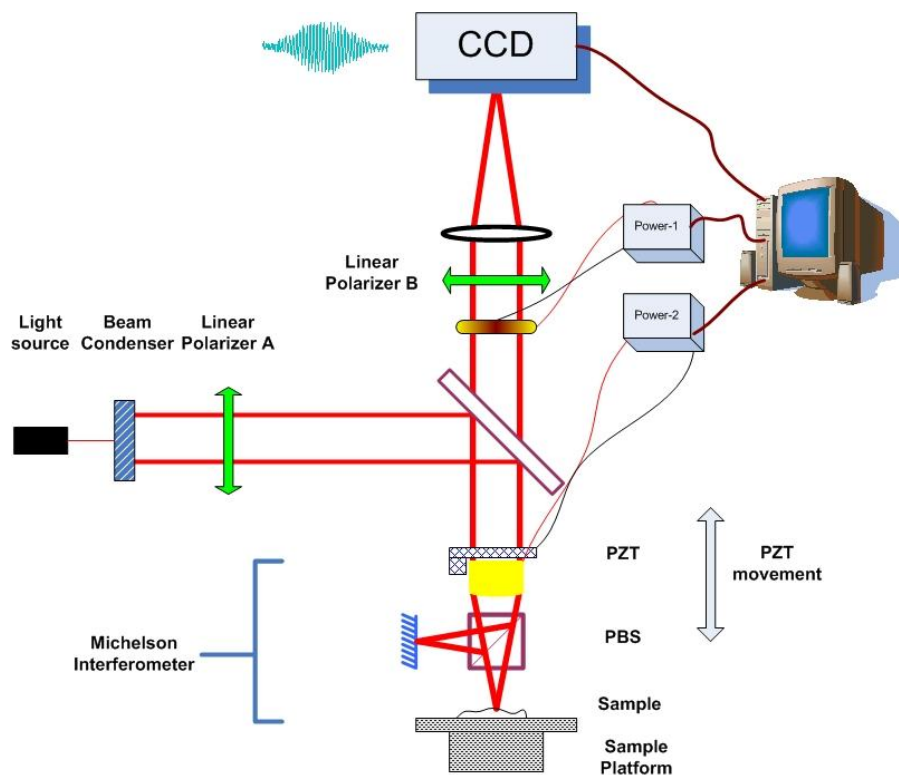


Figure 4. Schematic illustration of the Low Coherence Polarization Interference Microscope.

3.2. Measurement Mode and Algorithms

The relative phase profile between the object and reference beam is usually calculated using a phase shifting interferometry (PSI) algorithm.¹⁰ Continuing from the section (2.2), the intensity distribution on the CCD for each frame is given by

$$I_i(x, y) = I_o(x, y) + I_r(x, y) + 2\sqrt{I_o(x, y)I_r(x, y)} \cos [\phi(x, y) + \delta\phi(i)] \quad (3)$$

with $I_o(x, y)$ the object beam intensity and $I_r(x, y)$ the reference beam intensity. $\phi(x, y)$ is the relative phase shift between the object and reference beams and $\delta\phi(i) = \Gamma$ is the phase shift value varying from frame to frame. In this paper, the four frames algorithm is used. By rearranging the above equations the result of the phase map from the four step method is

$$\phi(x, y) = \tan^{-1} \left[\frac{I_4 - I_2}{I_1 - I_3} \right] \quad (4)$$

The modulation contrast $\gamma(x, y)$ at each pixel is calculated in accord with following expression,

$$\gamma(x, y) = \frac{I''}{I'} = \frac{2[(I_1 - I_3)^2 + (I_2 - I_4)^2]^{1/2}}{I_1 + I_2 + I_3 + I_4} \quad (5)$$

This value is useful for evaluating the quality of data that has been collected.

For thin objects whose discontinuities of adjacent pixels do not exceed $\lambda/4$, the surface information is readily obtained by PSI algorithm. For objects which have large step-like discontinuities, it is necessary to combine the PSI and vertical scanning interferometry¹¹ to solve the phase ambiguity problem¹². A piezoelectric transducer (PZT) for complimentary vertical scanning is introduced and is mounted onto the objective so that the best focus point on the object will move as the PZT moves. The system will work in the following way: first the best-focus frame position is obtained by locating the largest modulation-contrast position of the coherence envelope; second the phase shifting method is applied at each best-focus frame position. With this method, the time of generating the necessary data for further data processing will be a quarter or less of that of traditional vertical scanning because that the time consuming of Ceramic PM is negligible.

4. EXPERIMENTAL RESULTS

The experiments were carried out using the interference microscope introduced in section(3). The broadband light source has a center wavelength $633nm$. The magnification of the microscope objective and the eyepiece is $5X$ and $10X$ respectively. The fringes pattern were taken by an AVT MARLIN F-033B CCD camera with 640×480 pixels of $9.9\mu m \times 9.9\mu m$ size. The camera was connected to a computer through 1394 Firewire and grabs 14 frames/sec without any data processing.

Figure (5.a) presents four typical interference images that correspond to reference phase shifts of $\delta\phi(i) = 0, \pi/2, \pi, 3\pi/2$ using laser illumination for early alignment. The intensity variation of several pixels with reference phase changes from 0 to 5π is also plotted in figure (5.b). It was under broadband illumination. Our experiments have confirmed the feasibility of Ceramic PM working as a phase shifter. As a 3D object we chose a MEMS sample as large as $50\mu m \times 75\mu m \times 3\mu m$. To obtain the surface information of the sample, a PZT was used for complimentary vertical scanning. The PZT will travel at step of $0.633\mu m$ over a range of $5\mu m$ centered approximately on zero-order white light fringe. At each step, four measurements were made and the phase information will be calculated by the method introduced in section(3.2). The total computation and scanning time of this object is about $3s$. The three-dimensional representation obtained with the system is illustrated in figure (6). A more accurate surface profile could be obtained using signal-processing techniques, but are not of concern here.

5. CONCLUSION

In this paper we have introduced a new phase modulator called Ceramic PM. We have shown that this phase modulator has a short response time and great potential of being used in 3D imaging applications. At the same time a successful example of the application of Ceramic PM, LCPIM is discussed and several experimental results were presented. The performance of the system could be further improved by developing more advanced reconstruction algorithms.

The stability and achromatic properties of the Ceramic PM is under study. The fast response advantage of Ceramic PM will be appreciated more in 3D real time imaging for biology samples, where the demand for depth resolution is small and the response speed is more critical. Our further research effort will be directed to the application of Ceramic PM in wide field optical coherence tomography and hopefully a video-rate imaging system can be realized.

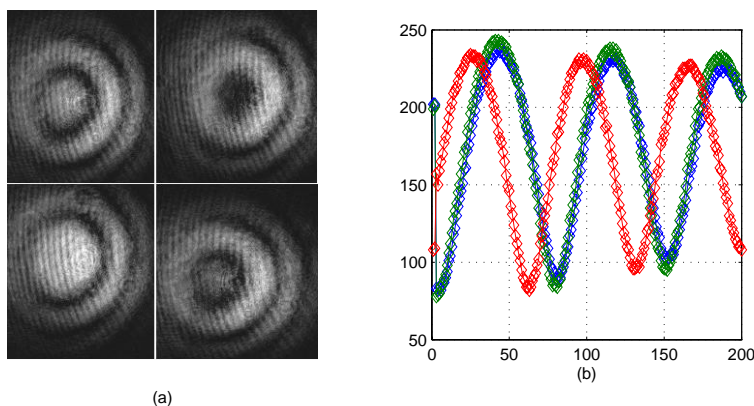


Figure 5. (a) four typical interference images that corresponds to reference phases shifts of $\delta\phi(i) = 0, \pi/2, \pi, 3\pi/2$, Laser illumination (b) The intensity variation of several pixels with reference phase changes from 0 to 5π

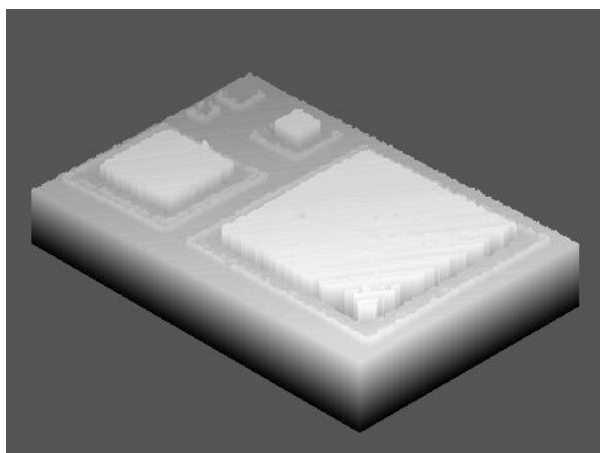


Figure 6. Three dimensional presentation of MEMS sample image. The size of the MEMES sample is $50\mu m \times 75\mu m \times 3\mu m$

REFERENCES

1. P. de Groot and L. Deck, "Three-dimensional imaging by sub-nyquist sampling of white light interferograms," *Opt. Lett.* **18**, pp. 1462–1464, 1993.
2. D. Huang, E. A. Swanson, C. Lin, J. S. Schuman, W. G. Stinson, W. Chang, M. Lee, T. Flotte, K. Gregory, C. A. Puliafito, and J. G. Fujimoto, "Optical coherence tomography," *Science* **254**, pp. 1178–1181, 1991.
3. I. Yamaguchi, T. Matsumura, and J. Kato, "Phase-shifting color digital holography," *Optics Letter* **27**, pp. 1108–1110, 2002.
4. de Groot P, C. de Lega X, K. J, and T. M., "Determination of fringe order in white-light interference microscopy," *Applied Optics* **41**, pp. 4571–4578, 2002.
5. M. Roy, C. J. R. Sheppard, and P. Hariharan, "Low-coherence interference microscopy using a ferro-electric liquid crystal phase-modulator," *Optical Express* **12**, pp. 2512–2516, 2004.
6. A. Zvyagin and D. Sampson, "Achromatic optical phase shiftermodulator," *Optics Letter* **26**, pp. 187–189, 2001.

7. E. Li, J. Yao, D. Yu, J. Xi, and J. Chicharo, "Optical phase shifting with acousto-optic devices," *Optics Letter* **30**, pp. 189–191, 2005.
8. H. Jiang, Y. Zou, and et al, "Transparent electro-optic ceramics and devices," in *Optoelectronic Devices and Integration*, H. Ming, X. Zhang, and M. Y. Chen, eds., *Proc. SPIE* **5644**, pp. 380–394, 2004.
9. B. Lee and T. Strand, "Profilometry with a coherence scanning microscope," *Appl. Opt.* **29**, pp. 3784–, 1990.
10. D. Malacara, *Optical Shop Testing*, Addison-Wesley, Reading, Mass., 1997.
11. K. Larkin, "Efficient nonlinear algorithm for envelope detection in white light interferometry," *J. Opt. Soc. Am. A* **13**, pp. 832–, 1996.
12. A. Harasaki, J. Schmit, and J. Wyant, "Improved vertical-scanning interferometry," *Appl. Opt.* **39**, pp. 2107–2115, 2000.